A Heart Arrhythmia Prediction Using Machine Learning's Classification Approach And The Concept Of Data Mining

[1] Roshani S Golhar, [2] Dr. Suraj V Pote, [3] Dr. Neerajkumar S Sathawane,

[1]*Research Scholar, Sunrise University, Alwar, Rajasthan, India.*
[2] *Associate Professor*
[3] *Associate Professor.*

Abstract:

Background and objectives:
According to the World Health Organisation, cardiovascular illnesses are the leading cause of mortality worldwide, killing around 17.9 million people each year. Arrhythmia is a type of cardiac illness characterised by a change in the linearity of the heartbeat. The purpose of this research would be to create new deep learning approaches for reliably interpreting arrhythmia using a single second segment. Because the ECG signal indicates unique electrical heart activity across time, considerable changes between time intervals are detected. Such variances, as well as the limited number of learning data available for each arrhythmia, make standard learning methods difficult, and so impede its exaggeration.

Conclusions*:*

The proposed method was able to outperform several state-of-the-art methods. Also proposed technique is an effective and convenient approach to deep learning for heartbeat interpretation, that could be probably used in real-time healthcare monitoring systems

Keywords

Electrocardiogram, ECG classification, Neural Networks(NNs), Convolutional neural networks (CNN), Portable Document Format (PDF)

Introduction:

Deep learning methods are increasingly being applied to electrocardiograms (ECGs), with recent studies indicating that neural networks (NNs) may predict future heart failure or atrial fibrillation based solely on the ECG. However, a huge number of ECGs are required to train NNs, and many ECGs are now only available in paper format, which is incompatible with NN training. We developed a completely automated online ECG digitization programme to transform scanned paper ECGs into digital signals. [12]. The programme automatically separates the ECG image into separate images for each of the 12 leads before applying a dynamical morphological approach to extract the signal of interest. The algorithm's performance was then tested using 1715 digitised ECGs from MIT BIH and clinical data. After removing ECGs with lead signal overlap, the automated digitisation technique achieved 99.0% correlation between the digitised signals and the ground truth ECG (n = 1715 standard 3by4 ECGs). We created and tested a fullyautomated, userfriendly online ECG digitization tool. Unlike other accessible programmes, this one does not

require human ECG signal segmentation[7]. Our solution can help with the quick and automated digitization of massive collections of paper ECGs so that they can be used in deep learning projects.

The application of machine learning to electrocardiograms (ECG) is gaining popularity. In general, wavelet analysis and local binary patterns were utilised to extract features from ECG, and subsequently support vector machine (SVM), k-nearest neighbour (kNN), and cutting-edge deep neural networks were investigated for arrhythmia detection. Convolutional neural networks (CNN) have also been used to identify incident heart failure by predicting the likelihood of Tachycardia and Bradycardia. Machine learning requires vast volumes of ECGs in electronic format, however in clinical practise, they are frequently printed on paper and are not available in digitised format[1]. Accessing and exploiting massive numbers of paper ECGs that have not been preserved electronically can be particularly difficult.Although ECG data sources are becoming more widely available, access to ECGs for machine learning applications would be substantially enhanced by an automated digitization tool capable of swiftly converting massive amounts of older paper-based ECGs into digital signals.

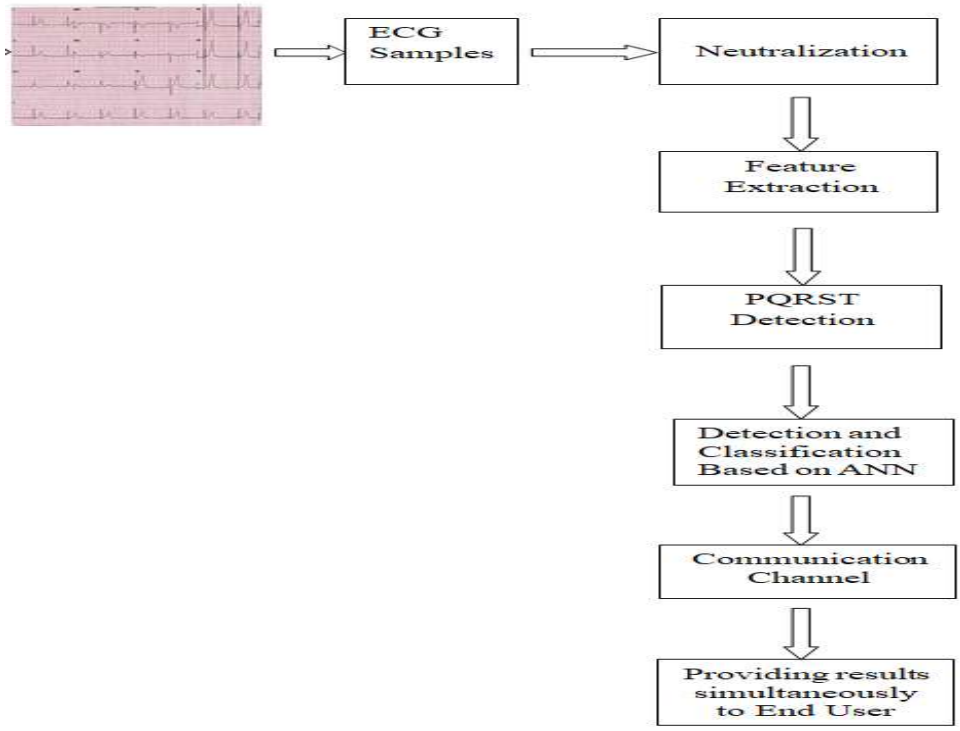

Figure 1. An explanation of the process used to digitise the automated ECG.

There have been several attempts to build 12-lead ECG digitization techniques. ECGscan, for example, was the first commercially available such tool, although it requires extensive human input to select the parts of the ECG that needed digitization[5]. Similarly, some digitization technologies require manual input to verify that the end-user accurately identifies the ECG leads. Others have created ECG digitization techniques that operate on segmented single-lead ECG images. Other efforts have been made to build automated digitisation techniques that do not require user input, but these algorithms can only digitise ECGs with leads printed in a specified arrangement.

Another method includes using a pre-set binary mask to extract the region of interest, albeit this method is limited to a single and specific arrangement of ECG data[22]. Furthermore, ECG digitization techniques for cardiac illness diagnosis and monitoring have been established. While no human intervention is required, no one method is applicable to all paper ECG formats. To validate, several current methods avoid directly comparing with the original digital ECG and instead use properties of the ECG such the PR, QRS, RR, QT intervals, or heart rate. A completely automated, user-friendly, accurate, and generalizable method for digitising paper electrocardiograms (ECGs) of varying configurations is lacking in the market. To overcome these limitations, we developed a public, hands-off method that can digitise 12-lead ECGs with signals produced in any standard configuration. We include this functionality into a user-friendly interface, and we anticipate that our tool will allow for the easy digitization of a large number of ECGs for machine learning applications.

Methods

Figure 1 depicts our algorithm for automated ECG digitization.Algorithms 17 in Supplementary material show the pseudocode for ECG digitization.The paper ECG image was initially preprocessed to remove any censored parts and grid lines before being turned into a binary image, allowing the ECG baselines to be recognised afterwards.After determining the ECG baselines, vertical anchor points were employed to determine the upper and lower boundaries of each ECG lead signal[2].This phase also helps the algorithm to decide the layout of the ECG leads on the printed ECG (i.e., the number of rows).Then, using lead name detection, the horizontal anchor points of each lead, i.e. the left- and right- hand limits of the ECG signals to be digitised, were utilised to crop and extract the signals in each lead of the 12-lead ECG. Finally, each lead's signals were digitised independently[9].

Source of development data.

Patients who came to Government Medical, Bhandara were recorded with 12-lead ECGs using hospital equipment; the bulk of our data originates from MIT-BIH. These ECGs were first printed on paper and then sent to the study team in the form of anonymized, scanned copies in Portable Document Format (PDF), which were then converted to 250 dpi Portable Network Graphics (PNG) files. Most of these electrocardiograms included three or four electrodes in lead II. There was no digital ECG ground truth data in this database; only paper ECGs were included. For the sake of developing and testing our digitization method[14] [27], we utilised only ECGs recorded at a paper speed of 25 mm/s and calibrated them to 1 mV = 10 mm.

Primary stage : . Pre-processing. All ECGs in the development database included a header made up of black pixels of censored patient information, which may have hampered digitisation of ECG traces. As a result, before beginning the digitization process, each ECG's censored area was automatically deleted. For each row, the average pixel intensity was zero in the blacked-out redacted area, but it was a positive scalar in the to-be-digitized parts of the image. This allowed the censored region to be reliably recognised and deleted before the ECG signals were digitised. ECGs are often printed on paper with gridlines that have been removed before to the digitization process. Given that the ECG contained red pixels, the image's red channel was set to 1 and the image was converted to greyscale. A threshold of 0.94 was employed to distinguish pixels from gridlines in the ECG signal. Pixels with values more than 0.94 were disregarded, while those with values less than 0.94 were considered to be indicative of an ECG signal or lead name. The ECG traces and lead name information were recovered from the binary image in this manner, and the backdrop and gridlines were removed. The processed binary image is depicted visually in Figures 2A, B.

ECG configuration determination and baseline detection. In the initial stage of automated digitization, the algorithm was required to identify the signal baseline and the number of rows of ECG signals in order to determine the ECG configuration[5]. Baselines in electrocardiograms (ECGs) were conceptualised as planes through which ECG signal strengths were maximally represented. To convert pictures from Cartesian to polar coordinates, the Hough transform is used. It has been put to use in the process of computing-vision feature extraction from digital images[9]. We employed the Hough transform to identify the ECG baselines. During the Hough transformation, two limitations were put in place to limit the amount of variables and prevent an incorrect identification of the baseline. Since the ECG baseline is often assumed to be horizontal, we started by only considering the x-axis values between +2.5 and -2.5. Second, any lines that were less than 80% of the width of the printed ECG were removed since the baseline is meant to span almost the full width of the picture. If the distance between adjacent ECG leads was less than 15% of the entire width of the picture, the lines were combined to create a single waveform. This guaranteed that adjacent leads' ECG signals remained separate and were not mixed throughout the digitization process. This method also assisted in determining the number of baselines on the printed ECG and, when combined with the vertical anchor point detection method described below, supplied information on lead configuration[14].

Next Step : Feature Extraction.

In the same way that baseline detection was used to generate vertical anchor points to identify ECG signals in space, vertical anchor points were utilised to define the upper and lower boundaries of the signals in each ECG lead in order to identify the signals to be digitised. The vertical cropping length is shown in Fig. 2B. For horizontal anchor point identification, higher and lower boundaries of 0.7 times the distance between two adjacent ECG signals (in the horizontal plane) above and below the ECG baseline were used. Horizontal anchor points were utilised to establish the left- and right-hand boundaries of the ECG signals to be digitised, which represented the start and end of the signals, respectively[4]. The start and end of the ECG signal to be digitised were the lead name and the start of the succeeding ECG signal in the horizontal

plane. For leads on the far right of the picture with no right-hand boundary, the maximum horizontal distance encompassing the ECG signal in other leads in the same ECG was utilised to establish the right-hand boundary When we were unable to detect lead names when they were close to the ECG baseline. ECG baselines were eliminated in these cases so that the digitisation tool could identify the lead names. In addition, morphological dilation and erosion were used on the image to improve the distinguishability of the lead names from the surrounding signals[19]. Both dilation and erosion are iterative region-growing techniques that thicken the lines, making it easier for automated procedures to recognise things of interest. All items of interest in the image were filtered with a width-height ratio greater than 5, as well as those with a width or height of 5 pixels or greater than 500 pixels.

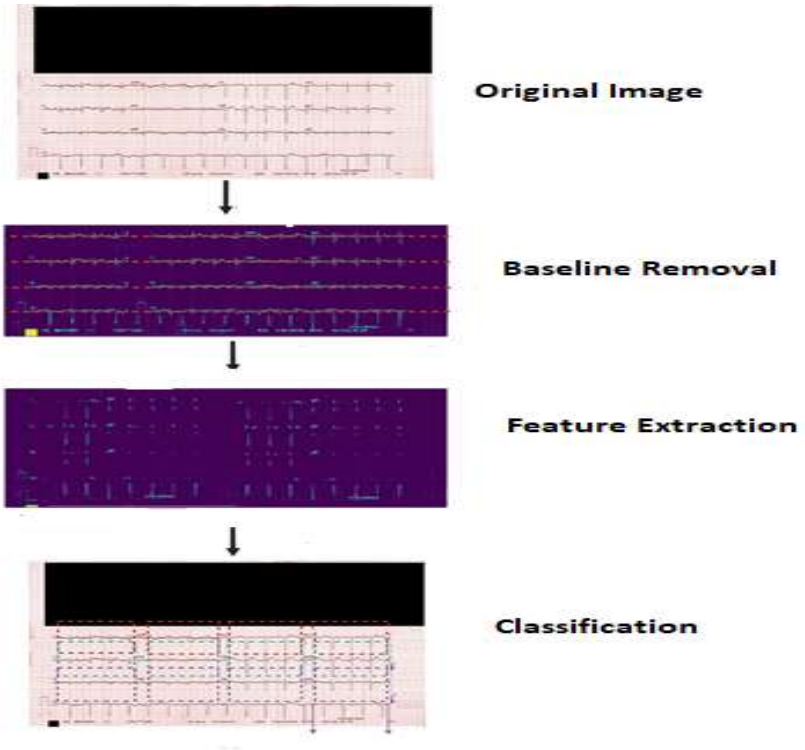

Figure 2. Image processing

The next step was to apply a deep learning model32 that had been trained on text character recognition to find the names of the main actors from the remaining filtered content. The model was fed a binary picture of a 12-channel electrocardiogram (ECG) and a set of ground-truth lead names ('I,' 'II,' 'III,' 'avr,' 'avl,' 'avf,' 'v1', 'v2', 'v3', 'v4', 'v5', 'v6') [11]. The result included any texts detected by the model, the text's related bounding box, and the confidence score. To discover lead names, confidence score thresholds were chosen so that the identification of one of the text strings resulted in a confidence score greater than the threshold. In this manner, lead name objects, as

well as their location, height, and breadth information, were identified for use as horizontal anchor points[17].

Step III: Extraction of a single lead ECG. To extract the ECG signals from the cropped image, "salt-and-pepper" noise, which consists of sparse white and black pixels, as well as any partial ECG signals from other leads, had to be removed[7]. This is especially true for high-amplitude ECG traces, which would intrude on the clipped pictures of adjoining leads, as illustrated in Fig. 3. To do this, we first employed picture dilation to connect any discontinuities in the ECG signal of interest, preventing any erroneous connections with noise or neighbouring signals. Following that, we regarded the image's largest discernible object to be the ECG signal of interest, and all other objects to be artefacts.

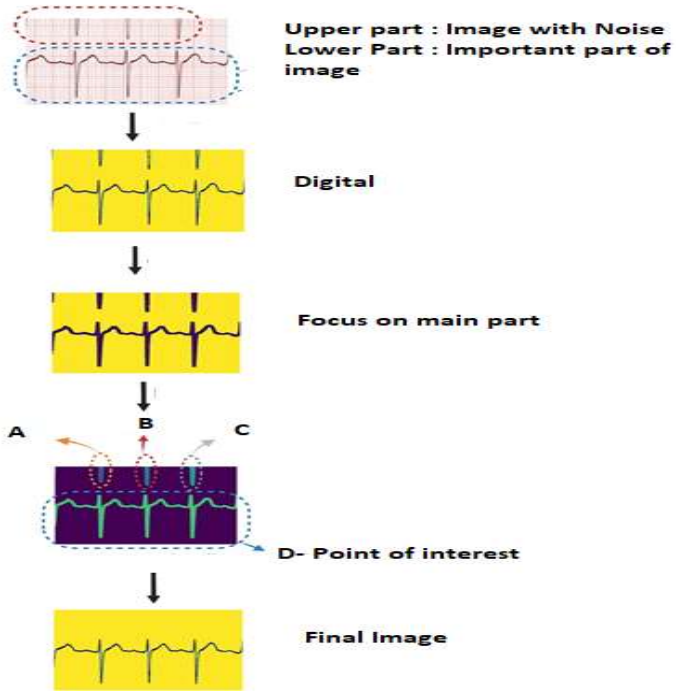

Figure 3. The procedure of preserving the signal of interest inside a cropped electrocardiogram (ECG).

Figure 3 shows how this strategy keeps the signal of interest while removing other objects from the cropped image.The retrieved ECG binary image was then converted into a one-dimensional digital ECG signal. In the binary image, the ECG signal is represented by a set of pixels with x (time) and y (voltage) coordinates calibrated at 25 mm/s and 10 mm/mv, respectively[6]. The matching amplitude along the x-axis of time may consist of many pixels. The median amplitude pixel (y-axis) of the binary picture was utilised to reconstruct the digital ECG signal since there

can only be one y-coordinate for each x-coordinate in the digital ECG signal. This produced a digitised ECG signal with pixel-level x and y coordinates. Using the rhythm (or longest signal) strip from each ECG, we were able to assign timestamps and voltage values to the digital ECG signal.. Given that the period of a conventional 12-lead ECG is 10 seconds, the time resolution was computed as 10 seconds divided by the number of pixels along the x-axis. Here voltage-time resolution ratio is standard at 0.1 mV/40 ms = 0.0025 mV/ms, with voltage-time resolution ratio (0.0025 mV/ms). Pixel count on the x-axis multiplied by time resolution, and pixel count on the y-axis multiplied by voltage resolution, were used to determine the timing and amplitude of the digital ECG signal, respectively. [1].

Final Stage: Development of an online dashboard tool. The web tool was created using Python dash plotly. The following stages provide end-users with step-by-step instructions for using the web tool. To begin, users must scan and upload an ECG image. All personal or patient-identifiable data should be thoroughly redacted and anonymized, users are advised. The picture is read by the Python method "cv2.imread" and can support any image format that "cv2.imread" supports. Following upload, the image is displayed with a set height of 600 pixels (px). Following that, a dropdown bar allows you to visualise each digitised ECG signal, with the opportunity to change the resolution by magnifying or reducing the screen[10] [22].

Statistical evaluations. The independent database collected from BIDMC was used for validation. Python was used to calculate Pearson's correlation and Root Mean Squared Error (RMSE) ("scipy.stat.pearsonr" for Pearson's correlation and "sklearn.metrics.mean_squared_error" for RMSE). P 0.001 was regarded as significant[13].

Result

Three distinct validation tests were used to validate our digitization tool. A database of paper ECGs was used to create the digitising technique. As a result, the parameters (QRS duration, PR, QT, and RR intervals) from these ECGs were the only way to validate our technology. To gain more accurate validation, we used an external ECG database from BIDMC that contained digital ECGs.

Validation 1: This validation was carried out using digital and paper ECGs that had been acquired.

Validation 2: ECG images by a cardiologist for validation.

Lead name	Correlation				Root mean squared error			
	Average	SD	*p*-value	Confidence interval: 97%	Average	SD	*p*-value	Confidence interval: 97%
I	0.991	0.016	< 0.001	0.967–0.979	0.043	0.033	< 0.001	0.031–0.036
II	0.992	0.007	< 0.001	0.924–0.945	0.033	0.027	< 0.001	0.037–0.043
V1	0.991	0.008	< 0.001	0.917–0.938	0.040	0.031	< 0.001	0.041–0.046
V2	0.991	0.007	< 0.001	0.937–0.955	0.044	0.030	< 0.001	0.048–0.055
V3	0.934	0.160	< 0.001	0.967–0.979	0.052	0.041	< 0.001	0.047–0.053
V4	0.988	0.014	< 0.001	0.896–0.921	0.090	0.102	< 0.001	0.083–0.096
V5	0.988	0.025	< 0.001	0.968–0.979	0.078	0.077	< 0.001	0.073–0.083
V6	0.991	0.018	< 0.001	0.961–0.972	0.062	0.064	< 0.001	0.058–0.066

Table 1. RMS and Correlation statistics (validation 3).

Lead name	Correlation				Root mean squared error			
	Average	SD	*p*-value	Confidence interval: 97%	Average	SD	*p*-value	Confidence interval: 97%
I	0.928	0.163	< 0.001	0.924–0.945	0.052	0.041	< 0.001	0.058–0.066
II	0.946	0.133	< 0.001	0.917–0.938	0.090	0.102	< 0.001	0.088–0.108
V1	0.973	0.092	< 0.001	0.989–0.992	0.078	0.077	< 0.001	0.049–0.056
V2	0.909	0.196	< 0.001	0.989–0.992	0.062	0.064	< 0.001	0.045–0.056
V3	0.974	0.085	< 0.001	0.896–0.921	0.044	0.030	< 0.001	0.064–0.078
V4	0.966	0.088	< 0.001	0.968–0.979	0.052	0.041	< 0.001	0.081–0.098
V5	0.952	0.134	< 0.001	0.961–0.972	0.050	0.038	< 0.001	0.083–0.096
V6	0.934	0.160	< 0.001	0.943–0.961	0.078	0.077	< 0.001	0.045–0.053

Table 2. RMS and Correlation statistics (validation 3).

Validation 3: ECG images and prints. Finally, the digitisation tool may be successfully used to both ECG images and paper scans of ECGs.

Discussion

We created a reliable and user-friendly online ECG digitising interface that can handle enormous amounts of paper ECGs. Its primary advantage is that it is totally automated and can be used to all printed ECGs regardless of lead design. After removing ECG images with lead signal overlap, validation on an external database of digital ECGs revealed 99.0% correlation and an average 0.04 mV RMSE on 8 ECG leads in a 3 by 4 layout. Here an average correlation of 95-97% across all leads. Due to lead signal overlapping, the average correlation of 12 by 1 ECG signals reduced to 50-70% in some leads. By changing the approach we successes in achieved 97% average correlation in 12 by 1 and 3 by

1 ECG.

Lead name	Correlation				Root mean squared error			
	Average	SD	*p*-value	Confidence interval: 97%	Average	SD	*p*-value	Confidence interval: 97%
I	0.125	0.209	< 0.001	0.606–0.670	0.073	0.078	< 0.001	0.126–0.152
II	0.116	0.078	< 0.001	0.690–0.757	0.063	0.894	< 0.001	0.088–0.112
V1	0.109	0.894	< 0.001	0.788–0.856	0.086	0.933	< 0.001	0.606–0.670
V2	0.772	0.933	< 0.001	0.126–0.152	0.139	0.209	< 0.001	0.690–0.757
V3	0.660	0.296	< 0.001	0.088–0.112	0.174	0.197	< 0.001	0.788–0.856
V4	0.638	0.078	< 0.001	0.606–0.670	0.168	0.261	< 0.001	0.606–0.670
V5	0.724	0.894	< 0.001	0.690–0.757	0.139	0.315	< 0.001	0.690–0.757
V6	0.822	0.933	< 0.001	0.788–0.856	0.100	0.296	< 0.001	0.788–0.856

Table 3. Correlation and root mean squared error (RMSE) statistics of selected 605 12 by 1 ECG pictures and ground truth digital ECGs before image thresholding (validation 2).

Lead name	Correlation				Root mean squared error			
	Average	SD	*p*-value	Confidence interval: 97%	Average	SD	*p*-value	Confidence interval: 97%
I	0.067	0.201	< 0.001	0.848–0.948	0.076	0.070	< 0.001	0.061–0.091
II	0.068	0.206	< 0.001	0.863–0.950	0.067	0.066	< 0.001	0.848–0.948
V1	0.898	0.235	< 0.001	0.061–0.091	0.068	0.095	< 0.001	0.048–0.088

Table 4. RMS and Correlation statistics (validation 3).

Lead name	Correlation				Root mean squared error			
	Average	SD	*p*-value	95% confidence interval	Average	SD	*p*-value	95% confidence interval
I	0.968	0.015	< 0.001	0.973–0.981	0.037	0.012	< 0.001	0.962–0.973
II	0.972	0.011	< 0.001	0.965–0.980	0.040	0.016	< 0.001	0.962–0.973
V1	0.963	0.013	< 0.001	0.957–0.982	0.037	0.011	< 0.001	0.962–0.973
V2	0.979	0.015	< 0.001	0.971–0.978	0.034	0.016	< 0.001	0.962–0.973
V3	0.973	0.056	< 0.001	0.969–0.977	0.037	0.024	< 0.001	0.962–0.973
V4	0.973	0.052	< 0.001	0.957–0.988	0.037	0.025	< 0.001	0.032–0.047
V5	0.971	0.013	< 0.001	0.983–0.990	0.034	0.024	< 0.001	0.031–0.042
V6	0.988	0.006	< 0.001	0.990–0.993	0.037	0.015	< 0.001	0.029–0.038

Table 5. RMS and Correlation statistics (validation 3).

Lead name	Correlation				Root mean squared error			
	Average	SD	*p*-value	95% confidence interval	Average	SD	*p*-value	95% confidence interval
I	0.942	0.027	< 0.001	0.935–0.950	0.049	0.017	< 0.001	0.045–0.054
II	0.971	0.015	< 0.001	0.967–0.975	0.045	0.023	< 0.001	0.038–0.051
V1	0.988	0.009	< 0.001	0.985–0.990	0.031	0.011	< 0.001	0.028–0.034

Table 6. RMS and Correlation statistics (validation 3).

Lead name	Correlation				Root l			
	Average	SD	*p*-value	95% confidence interval	Average	SD	*p*-value	95% confidence interval
I	0.968	0.016	< 0.001	0.035–0.043	0.968	0.016	< 0.001	0.962–0.973
II	0.972	0.014	< 0.001	0.029–0.038	0.968	0.016	< 0.001	0.957–0.988
V1	0.968	0.013	< 0.001	0.026–0.032	0.968	0.016	< 0.001	0.983–0.990
V2	0.968	0.025	< 0.001	0.028–0.038	0.968	0.016	< 0.001	0.990–0.993
V3	0.968	0.042	< 0.001	0.026–0.032	0.968	0.016	< 0.001	0.957–0.988
V4	0.968	0.012	< 0.001	0.028–0.038	0.968	0.016	< 0.001	0.962–0.973
V5	0.968	0.013	< 0.001	0.030–0.044	0.968	0.016	< 0.001	0.957–0.988
V6	0.974	0.014	< 0.001	0.035–0.043	0.968	0.016	< 0.001	0.962–0.973

Table 7. RMS and Correlation statistics (validation 3).

By changing the approach to digitizing of ECG signal extraction the numerous features can be fetches and identified which will help to strengthen the prediction. We use connection algorithms to name and remove tiny objects, same as other digitization interfaces[28].

The goal for developing our application was to enable users to rapidly and easily produce huge volumes of digital ECGs from their paper, picture, or scanned counterparts. We anticipate that this will be especially valuable for people who want to use ECGs in machine learning applications. Although this can be accomplished without digitising ECGs, such as with paper

ECGs or their photographs, the quality of the output is essentially dictated by the quality of the input.

Overall benefits of the designed system are:

1. It is totally automated, requiring no manual user input for single lead signal segmentation.

2. A novel approach of text base method applicable to different ECG image configurations.

3. A quick digitalization at the moment of need is enabled by an effective ECG extraction technique.

The following are the limitations:

Because our text recognition algorithm was trained on generic photos, lead names on printed ECGs may not always be recognised. For example, if the leads I, II, and III are masked by high voltage ECG signals, the instrument may not be able to detect them accurately. Lead name detection may be imprecise in pixelated and low-resolution ECGs.

Conclusion

We created a verified, fully-automated, user-friendly online 12-lead ECG digitisation tool that demonstrates a high level of accuracy and reliability when compared to external validation datasets. It is made up of many logic-based modules and a comprehensive text character recognition deep learning model, allowing it to be applied to all common ECG setups in various clinical contexts. It can also be used on printed and/or scanned ECGs, allowing for large-scale digitization of paper ECGs with no user input.

Reference Data

In our project the data is available on MIT BIH website and also we can generate the data at clinic as we generated here at Government Medical Bhandara.

References

1 .Neerajkumar Sathawane, U. M. Gokhale. Inception based GAN for ECG arrhythmia classification. International Journal of Nonlinear Analysis and Applications 12, 1585-1594 (2021).

2. Neerajkumar Sathawane, U. M. Gokhale. Design of Cardiovascular Disease Classification Using Wavelet Transform and Detection Using Neural Network. ICT Analysis and Applications: Proceedings of ICT4SD 2020, Volume 2, 35-44 (2021)

3. Tuncer,& others. A paper based on wavelet transform with ECG signals. Knowl. Based Syst. 186, 104923 (2019).

4. Subasi, A. & others A paper basd on NN and deep learning. J. Ambient Intell. Human. Comput.https://doi.org/10.1007/s12652-021-03324-4 (2021).

5. Baygin, & others. Automatic arrhythmia detection in ECG records. Inf. Sci. 575, 323–337 (2021).

6. Kobat and others: An ECG signal classification using learning architecture. Symmetry 13, 1914 (2021).

7. Attia, Z. I. et al. A paer based on sinus rhythm for outcome prediction. Lancet 394, 861–867 (2019).

8. Raghunath, S. et al. Paper based on DNN for stroke. Circulation 143, 1287–1298 (2021).

9. Khurshid, S. et al. ECG-based atrial fibrillation. Circulation 145, 122–133 (2022).

10. Attia, Z. I. et al.Paper based on AI for scanning ECG. Nat. Med.

25, 70–74 (2019).

11. Adedinsewo, D. et al.Paper based on Ai for heart arrhythmia. Circ. Arrhythmia Electrophysiol. 13, e008437 (2020).

12. Akbilgic, O. et al. ECG-AI: Eur. Heart J. Digit. Health 2, 626–634 (2021).

13. Kwon, J.-M. et al. A paper based on AI for electrocardiographic features. Eur. Heart J. Digit. Health 2, 106–116 (2021).

14. Grün, D. et al. A paper based on: a meta-analysis. Front. Digit. Health 2, 584555 (2021).

15. Cho, J. et al. Paper based on AI fraction using electrocardiography.ASAIO J. 67, 314–321 (2021).

16. Ko, W.-Y. et al. Detection of hypertrophic cardiomyopathy using a CNN-enabled ECG. J. Am. Coll. Cardiol. 75, 722–733 (2020).

17. Rahman, Q. A. et al. Paper based on ECG-based heartbeat. IEEE Trans. Nanobiosci. 14, 505–512 (2015).

18. Galloway, C. D. et al. Paper based of deep-learning model for the the electrocardiogram.JAMA Cardiol. 4, 428–436 (2019).

19. Cohen-S, M. et al. ECG using artificial intelligence. Eur. Heart J. 42, 2885–2896 (2021).

20. Kwon, J.-M. et al. Paper based on deep learning for ECG. J. Am. Heart Assoc. 9, e014717 (2020).

21. Kwon, J.-M. et al. AI for ECG. J. Electrocardiol. 59, 151–157 (2020).

22. Badilini & others. J. ECGSCAN: a paper based on electrocardiographic printouts. J. Electrocardiol. 38, 310–318 (2005).

23. Ravichandran, L. et al. Based on ECG. IEEE J. Transl. Eng. Health Med. 1, 1800107–1800107 (2013).

24. Fortune, J., Coppa,q & others. Digitizing ECG image. medRxiv (2021).

25. Mishra, S. et al. Paper based on ECG paper record. J. Med. Biol. Eng. 41, 422–432 (2021).

26. Mallawaarachchi, & others for extracting ECG signals from scanned trace reports. In IEEE Conference IECBES, 868–873 (IEEE, 2014).

27. Shi, G., Zheng, G. & Dai, Paper based on k-means method. In CC, 797–800 (IEEE, 2011).

28. Swamy, P., Jayaraman, S. & Chandra, M. G. A digital time series signal generation for ECG records. In ICBBT, 400–403 (IEEE, 2010).

29. Baydoun, M. et al. A step toward machine learning. IEEE J. Transl. Eng. Health Med. 7, 1–8 (2019).

30. Isabel and others, Electrocardiogram printed records for mobile app by deep-learning-based classification. In Computing in Cardiology (CinC), vol. 48, 1–4 (IEEE, 2021).

31. Sangha, V. et al. Paper based on electrocardiographic images and signals. Nat. Commun. 13, 1–12 (2022).

32. Hough and others. US Patent 3,069,654.

33. Lobodzinski,& others. Paper based on hard copy electrocardiograms.

J. Electrocardiol. 36, 151–155 (2003).

34. Li, Y. et al. Paper-based ECG. Comput. Biol. Med. 127, 104077 (2020).